



A Novel Validated Recurrence Stratification System Based on ¹⁸F-FDG PET/CT Radiomics to Guide Surveillance After Resection of Pancreatic Cancer

Miaoyan Wei^{1,2,3,4,5†}, Bingxin Gu^{3,6,7†}, Shaoli Song^{3,6,7}, Bo Zhang^{1,2,3,4,5}, Wei Wang^{1,2,3,4,5}, Jin Xu^{1,2,3,4,5}, Xianjun Yu^{1,2,3,4,5*} and Si Shi^{1,2,3,4,5*}

OPEN ACCESS

Edited by:

Claudio Florino,
San Raffaele Hospital (IRCCS), Italy

Reviewed by:

Concetta Piazzese,
University of Huddersfield,
United Kingdom
Hsin Wu Tseng,
University of Arizona, United States

*Correspondence:

Xianjun Yu
yuxianjun@fudanpci.org
Si Shi
shisi@fudanpci.org

[†]These authors have contributed
equally to this work

Specialty section:

This article was submitted to
Cancer Imaging and
Image-directed Interventions,
a section of the journal
Frontiers in Oncology

Received: 06 January 2021

Accepted: 19 April 2021

Published: 12 May 2021

Citation:

Wei M, Gu B, Song S, Zhang B,
Wang W, Xu J, Yu X and Shi S
(2021) A Novel Validated Recurrence
Stratification System Based on
¹⁸F-FDG PET/CT Radiomics
to Guide Surveillance After
Resection of Pancreatic Cancer.
Front. Oncol. 11:650266.
doi: 10.3389/fonc.2021.650266

¹ Department of Pancreatic Surgery, Fudan University Shanghai Cancer Center, Shanghai, China, ² Pancreatic Cancer Multidisciplinary Center, Fudan University Shanghai Cancer Center, Shanghai, China, ³ Department of Oncology, Fudan University Shanghai Medical College, Shanghai, China, ⁴ Pancreatic Cancer Institute, Fudan University, Shanghai, China, ⁵ Shanghai Pancreatic Cancer Institute, Shanghai, China, ⁶ Department of Nuclear Medicine, Fudan University Shanghai Cancer Center, Shanghai, China, ⁷ Center for Biomedical Imaging, Fudan University, Shanghai, China

objective: Despite the heterogeneous biology of pancreatic cancer, similar surveillance schemas have been used. Identifying the high recurrence risk population and conducting prompt intervention may improve prognosis and prolong overall survival.

Methods: One hundred fifty-six resectable pancreatic cancer patients who had undergone ¹⁸F-FDG PET/CT from January 2013 to December 2018 were retrospectively reviewed. The patients were categorized into a training cohort (n = 109) and a validation cohort (n = 47). LIFEx software was used to extract radiomic features from PET/CT. The risk stratification system was based on predictive factors for recurrence, and the index of prediction accuracy was used to reflect both the discrimination and calibration.

Results: Overall, seven risk factors comprising the rad-score and clinical variables that were significantly correlated with relapse were incorporated into the final risk stratification system. The 1-year recurrence-free survival differed significantly among the low-, intermediate-, and high-risk groups (85.5, 24.0, and 9.1%, respectively; p < 0.0001). The C-index of the risk stratification system in the development cohort was 0.890 (95% CI, 0.835–0.945).

Conclusion: The ¹⁸F-FDG PET/CT-based radiomic features and clinicopathological factors demonstrated good performance in predicting recurrence after pancreatectomy in pancreatic cancer patients, providing a strong recommendation for an adequate adjuvant therapy course in all patients. The high-risk recurrence population should proceed with closer follow-up in a clinical setting.

Keywords: ¹⁸F-FDG PET/CT, radiomic features, pancreatic cancer, recurrence, surveillance

INTRODUCTION

Pancreatic ductal adenocarcinoma (PDAC) is a fatal malignancy with a 5-year overall survival less than 9% (1). Early detection of pancreatic cancer remains challenging; radical surgical resection offers the only chance of cure, and at best, only 20% are suitable for curative resection in newly diagnosed patients (2). Despite considerable improvements in surgery, the overall survival (OS) of these resected cases remains poor, and the recurrence rate is 80%. The previous study identified a recurrence-free interval of 12 months as the optimal cutoff in pancreatic cancer to distinguish early and late recurrence (3). Data on the roles of surveillance in patients with resected PDAC are limited, and similar surveillance schedules are applied after resection for all pancreatic cancers despite their heterogeneous biology. Specifically, carbohydrate antigen 19-9 (CA19-9) measurements and contrast-enhanced computed tomography (CT) every 3 to 6 months for 2 years after radical resection are recommended according to the latest version of the National Comprehensive Cancer Network (NCCN) guidelines. The expert opinion of French clinical practice guidelines proposed that the evaluation and surveillance of patients after curative resection to monitor relapse at an early stage should be performed every 3 months over 2–3 years, and then every 6–12 months up to 5 years (4). Therefore, establishing a recurrence stratification system to guide surveillance of resected pancreatic cancer (RPC) patients is urgent need in this field.

In diagnosing of pancreatic cancer, CT is the first-line imaging approach used to determine the resectability according to the NCCN criteria to predict R0 resection. Secondary signs, including pancreatic duct dilatation, are vital to diagnose PDAC (5). Pancreatic cancer cells have extensively reprogrammed metabolism, and the most useful aspect of ^{18}F -positron emission tomography/CT (^{18}F -PET/CT) is that it adds precise anatomical localizations to functional data. Thus, ^{18}F -PET/CT plays superior diagnostic roles in evaluating the stage, determining the therapy response, predicting survival and detecting recurrence compared with conventional imaging (6–9). Its value in predicting distant metastasis and survival likely originates from the strong correlation between the levels of fluorodeoxyglucose (FDG) uptake and tumor aggressiveness in terms of the pathological grade (10). For resected PDAC patients, ^{18}F -FDG PET/CT metabolic parameters, including the maximum standardized uptake value (SUV_{max}), total lesion glycolysis, and metabolic tumor volume, are significantly associated with OS or disease-free survival (11), indicating that PET/CT scan activity may act as a prognostic factor after pancreatectomy, consistent with the conclusion that glucose metabolic pathways are crucial in PDAC biology.

As a non-invasive, data-characterization algorithms that assesses the spatial heterogeneity of volumes of Interest (VOIs) in medical imaging, texture analysis of tumors has attracted increased interest (12). Radiomics has emerged in this context and is the most advanced in application within the medical field of oncology, which extracts high-throughput features from radiographic medical images and provides insight into the underlying innate biology of tumors. These features, termed radiomic features, may be useful for improving the predictive

accuracy and therapeutic response for various conditions of the disease, potentially uncovering the valuable disease characteristics for personalized therapy (13). The radiomic features of PDAC have been investigated recently, identifying prognostic intratumor heterogeneity or predicting survival intervals and treatment responses based on CT, MRI, or PET/CT radiomic features (14–18), which could optimize treatment strategies and facilitate individualized therapy in this field. Here, we postulated that combining ^{18}F -FDG PET/CT radiomic features and clinicopathological characteristics could reflect the properties of pancreatic tumors and may provide valuable information to improve prognostic prediction. Therefore, this study aimed to establish a recurrence risk stratification system for initially resectable PDAC patients after pancreatectomy to better guide monitoring and surveillance in a clinical setting.

MATERIALS AND METHODS

Patient Selection

Consecutive resectable patients with histopathologically confirmed PDAC who had undergone preoperative ^{18}F -FDG PET/CT followed by radical pancreatectomy between January 2013 and December 2018 at the Department of Pancreatic Surgery, Shanghai Cancer Center, were included. The criteria defining the resectability status at diagnosis were made by multidisciplinary discussions based on the NCCN guidelines. Additionally, all the patients in the cohort had undergone a pancreatic protocol CT for staging and the determination of local resectability. Only initially resectable patients were included in this study.

^{18}F -FDG PET/CT imaging was performed within 15 days before surgery and without antitumor treatment received within at least 2 years before the examination. The exclusion criteria of our study were as follows: (1) malignancy other than pancreatic cancer was present; (2) a tumor site with low-grade ^{18}F -FDG uptake (less than 2.5); (3) the primary tumor was too small for accurate texture analysis; (4) an R2 surgical margin; and (5) postsurgical radiotherapy. The data collected included patient demographics, PET/CT slices, metabolic activity parameters, CA19-9 levels, pathological parameters, adjuvant therapy regimen and number of cycles. Specifically, preoperative CA19-9 was measured within 7 days before surgery and 4–6 weeks postoperatively. Recurrence in our cohort included both local and distant disease relapses.

One hundred fifty-six PDAC patients were enrolled according to the above criteria, and the patients were divided into two cohorts based on the time of consultation, with 109 patients assigned to the development set (from 2013.01 to 2016.12) and 47 assigned to the validation set (from 2017.01 to 2018.12). The study was approved by the institutional ethics committee.

^{18}F -FDG PET/CT Scan Protocol and Image Acquisition

^{18}F -FDG PET/CT scans were performed using a Siemens CTI RDS Eclipse ST system (Knoxville, Tennessee, USA). The enrolled patients were asked to fast for at least 6 h and

presented blood glucose levels less than 8 mmol/L at the injection of ^{18}F -FDG (7.4 MBq/kg body weight) intravenously. Image acquisition started 60 ± 5 min following the tracer administration. The CT acquisition parameters were as follows: tube voltages: 120 kV, tube current: 80–250 mA, slice thickness: 5.0 mm, pitch: 1.0 mm, rotation time: 0.5 s. PET was acquired with 2–3 min per table position. PET image data sets were reconstructed iteratively using an ordered-subset expectation maximization iterative reconstruction (OSEM) by applying CT data for attenuation correction. The reconstruction parameters were as follows: iterations: four, subsets: eight, pixel size: 4.0×4.0 mm, zoom: 1.0, full width half maximum (FWHM): 6.0 mm, and slice thickness: 5.0 mm. PET scanning and a low-dose CT scans were then performed immediately. The PET images were acquired using CT-based attenuation correction. The ordered-subsets expectation maximization technique was adopted to reconstruct the PET data—specifically, a 168×168 image matrix with eight subsets and four iterations. Coregistered scans were displayed on a workstation.

VOI Drawing, Radiomic Feature Extraction and Image Analysis

To extract the PET/CT imaging texture features of the lesions, we applied LIFEx software (v4.00, <http://www.lifexsoft.org>). PET and CT images in the DICOM format were consecutively imported into LIFEx and automatically fused by the software. Areas with abnormal uptake of ^{18}F -FDG on PET and abnormal density on CT were defined as lesions. The final VOI of the primary tumor lesion was automatically defined on PET images with a threshold of 40% of the SUVmax. We performed VOI placement for attenuation correction of low-dose CT images from the PET/CT scan. Then, the spatial resampling was implemented as 2 mm in spacing X, Y, and Z on both PET and CT images by three-dimensional Lagrangian polygon interpolation for all 156 patients. Using a threshold of 40% of the SUVmax, two experienced PET/CT diagnostic physicians semiautomatically delineated the VOI of the target lesion. Texture features were calculated only for VOIs of ≥ 64 voxels because textural features cannot be accurately quantified for small regions. The PET and CT features were then automatically extracted from the same VOI, and 94 radiomic features were extracted using LIFEx software. Four gray-level matrices were calculated in three dimensions, giving 46 radiomics features (including first-order and second-order features and volumes) for each of the CT-tumor VOIs and 48 radiomics features for each of the PET-tumor VOIs. The radiomic feature extraction process is shown in **Figure 1**. All 94 features are shown in the supplementary material (**Table S1**). Particularly, the forty-eight conventional PET parameters and radiomics features were extracted and in agreement with the IBSI description, including:

- Eight conventional PET parameters: SUVmax, SUVmean, SUVmin, SUVpeak, SUVstd, SUVskewness, SUVkurtosis, and TLG
- Six descriptors of the image intensity histogram: HISTO_Skewness (asymmetry), HISTO_Kurtosis (flatness),

HISTO_ExcessKurtosis, HISTO_Energy (uniformity), HISTO_Entropy_log2, and_log10 (randomness);

- Two shape-based features, that describe shape and compact of VOI: SHAPE_Sphericity, and SHAPE_Compacity;
- Thirty-two textural features: (a) seven features from gray-level co-occurrence matrix (GLCM): describing the correlation between pair of voxels in 13 directions of a three-dimensional space; (b) eleven features from gray-level run length matrix (GLRLM): describing the number and length of run with a certain level of gray in 13 directions of a three-dimensional space; (c) eleven features from gray-level zone length matrix (GLZLM): describing the number and size of zone with a certain level of gray in 13 directions of a three-dimensional space; (d) three features from neighborhood gray-level different matrix (NGLDM): describing the difference between a voxel and its connected neighbors.

46 features from CT including:

- Six conventional CT parameters: HUmax, HUmean, HUmin, HUstd, HUSkewness, and HUKurtosis
- Six descriptors of the image intensity histogram: HISTO_Skewness, HISTO_Kurtosis, HISTO_ExcessKurtosis, HISTO_Energy, HISTO_Entropy_log2, and_log10;
- Two shape-based features: SHAPE_Sphericity, and SHAPE_Compacity;
- Thirty-two textural features that consistent with PET features.

All the texture features were summarized and defined in detail in the **Supplemental Materials**.

Radiomic Feature Screening and Score Model Establishment

The optimum features were selected from the radiomic features to establish a radiomic model in the training cohort. Next, we used the least absolute shrinkage and selection operator (LASSO) algorithm to screen the optimal predictive features among 94 radiomic features in the development cohort. The radiomic signature score (rad-score) was calculated according to the selected radiomic features of each patient. In this study, we employed the receiver operating characteristic (ROC) and the area under the curve (AUC) to assess the performance of the model in the development set that was verified in the validation set.

Patient Clinicopathological Characteristics, Treatment Variables and Follow-up

The relevant patient clinicopathological factors included age, sex, body mass index (BMI), the preoperative neutrophil-to-lymphocyte ratio (NLR), the platelet-to-lymphocyte ratio (PLR), and the serum CA19-9 level. The perioperative complications within 90 days of surgery were graded using the Clavien-Dindo classification. The data on the tumor size, differentiation grade, lymph node metastasis, lymphovascular invasion (LVI), perineural invasion (PNI), Ki-67 index and SMAD4 expression by immunohistochemistry were collected.

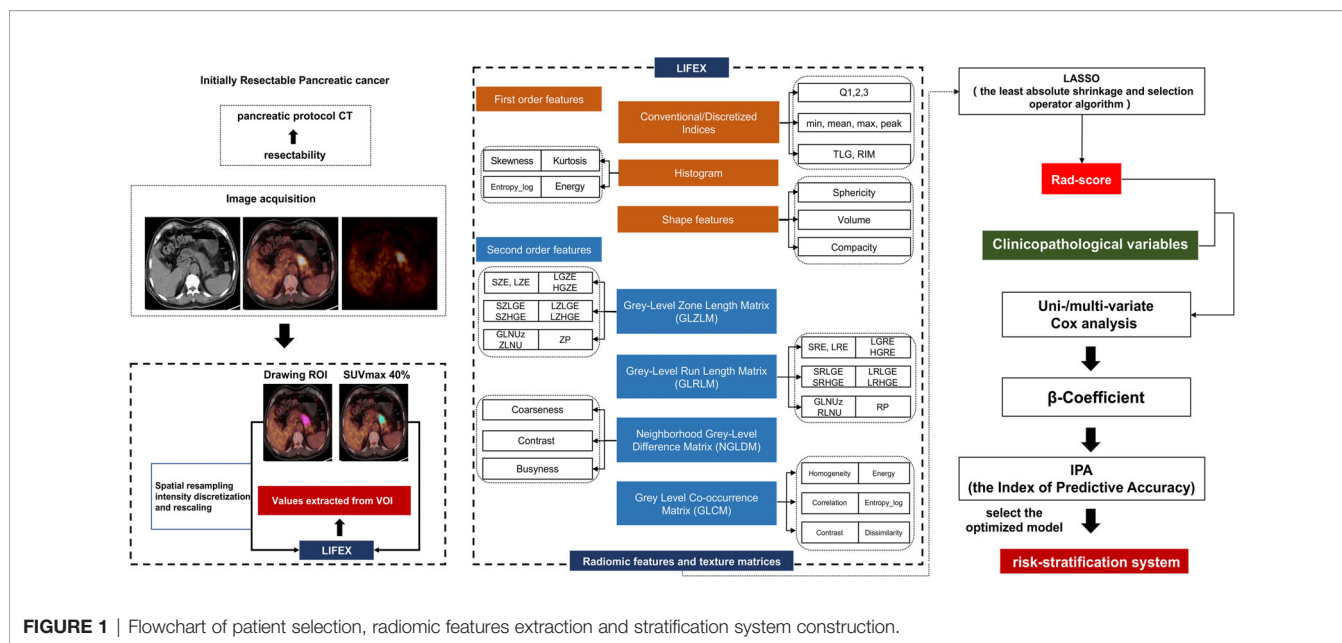


FIGURE 1 | Flowchart of patient selection, radiomic features extraction and stratification system construction.

Postoperative data including the timing, regimen and cycles of adjuvant chemotherapy were collected. Pathological T and N stages were classified according to the American Joint Committee on Cancer (AJCC) staging guidelines 8th edition. All the patients had undergone clinical follow-up that included imaging studies (contrast-enhanced CT were required) and blood tests. Clinical evidence of no recurrent disease comprised negative findings on regular imaging and no incremental increase in tumor markers. Recurrence-free survival (RFS) included any recurrence (local or regional, or distant) and death due to any cause.

Statistical Analysis

Statistical analyses were implemented in R software (version 3.4.3; <http://www.R-project.org>, R Foundation for Statistical Computing, Vienna, Austria) and SPSS Statistics (version 23.0; IBM, Armonk, NY, USA). To compare continuous variables, we adopted independent samples t or the Mann–Whitney U test, while chi-squared test was used to compare categorical variables. The LASSO algorithm was applied to further identify the optimal features and build the radiomic features score (rad-score) (19–21). A Cox proportional hazards regression model was employed to recognize independent recurrence predictors and calculate hazard ratios (HRs), 95% confidence intervals (CIs), and β regression coefficients. Variables that were statistically significant in univariate analysis were included in multivariate analysis and the risk stratification system ($P < 0.05$). Inspired by Sullivan et al. (22), the β -coefficients of each covariate from the Cox proportional hazards regression model were used to generate an integer-based point scoring system for each covariate; the overall score was calculated as the sum of the covariate weighted scores. By dividing the β coefficients with the constant values of the largest β coefficient in the final model, scores were assigned and multiplied by 10 and rounded to the nearest integer. To select

an optimized model, the index of predictive accuracy (IPA) was employed and realized by the IPA function in the “risk regression” package in R (23). As a new bio-informatics tool for biomarker assessment and outcome-based cut-point optimization, X-Tile plot provides a single, global assessment of every possible way of dividing a population into low-, medium-, and high-level marker expression. In our study, X-tile plot was used to generate the optimum cutoff point of risk score according to the highest χ^2 -value defined by Kaplan–Meier survival analysis and log-rank test (Figure S1). X-tile data are presented in a right triangular grid where each point represents a different cut-point. The intensity of the color of each cutoff point represents the strength of the association. The values of risk score were used as input for the X-Tile plots. The groups were divided into low-, intermediate-, and high-risk groups according to cutoff values of risk score (24). The survival of RFS was estimated using the Kaplan–Meier method and compared using the log-rank test. A P value < 0.05 was considered statistically significant.

RESULTS

Baseline Clinical Characteristics of the Patients

Of the 156 enrolled resected pancreatic cancer patients, 92 were male, accounting for nearly 60%; the mean age was 61.54 ± 8.37 years. The overall median postsurgical follow-up period was 24.8 months (range, 3–84.8). All the resected patients received adjuvant chemotherapy, and 106 (67.5%) patients had recurrence. Regarding tumor pathology, most of the patients had moderate to low differentiation, with high differentiation in 22 patients (14.1%). A total of 52.6% of patients presented with positive lymph node metastases. Additionally, 42.9% of pancreatic cancer patients had a CA19-9 reduction $\geq 80\%$ compared with the

TABLE 1 | Clinical characteristics of resectable pancreatic cancer patients at baseline in the training and validation cohorts.

Variables	Overall (N = 156)	Training cohort (N = 109)	Validation cohort (N = 47)	P
Sex				1
Female	64 (41.0%)	45 (41.3%)	19 (40.4%)	
Male	92 (59.0%)	64 (58.7%)	28 (59.6%)	
Age (years)				0.527
>60	92 (59.0%)	62 (56.9%)	30 (63.8%)	
≤60	64 (41.0%)	47 (43.1%)	17 (36.2%)	
BMI (kg/m ²)				0.604
<18.5	15 (9.6%)	10 (9.2%)	5 (10.6%)	
18.5–24.9	102 (65.4%)	75 (68.8%)	27 (57.4%)	
25–28	28 (17.9%)	17 (15.6%)	11 (23.4%)	
28–32	10 (6.4%)	6 (5.5%)	4 (8.5%)	
>32	1 (0.6%)	1 (0.9%)	0 (0.0%)	
Operation				0.942
DP	76 (48.7%)	54 (49.5%)	22 (46.8%)	
PD	71 (45.5%)	49 (45.0%)	22 (46.8%)	
TP	9 (5.8%)	6 (5.5%)	3 (6.4%)	
NLR				0.562
≥5	15 (9.6%)	9 (8.3%)	6 (12.8%)	
<5	141 (90.4%)	100 (91.7%)	41 (87.2%)	
PLR				0.650
≥110	114 (73.1%)	78 (71.6%)	36 (76.6%)	
<110	42 (26.9%)	31 (28.4%)	11 (23.4%)	
ΔCA19-9 decrease				0.128
<80%	89 (57.1%)	67 (61.5%)	22 (46.8%)	
≥80%	67 (42.9%)	42 (38.5%)	25 (53.2%)	
R status				0.622
R0	124 (79.5%)	85 (78.0%)	39 (83.0%)	
R1	32 (20.5%)	24 (22.0%)	8 (17.0%)	
Tumor differentiation				0.667
High	22 (14.1%)	14 (12.8%)	4 (8.5%)	
Median	95 (60.9%)	74 (67.9%)	32 (69.1%)	
Low	39 (25.0%)	21 (19.3%)	11 (23.4%)	
T stage				0.451
1	25 (16.0%)	15 (13.8%)	10 (21.3%)	
2	89 (57.1%)	65 (59.6%)	24 (51.1%)	
3	42 (26.9%)	29 (26.6%)	13 (27.7%)	
N stage				0.786
0	74 (47.4%)	56 (51.4%)	26 (55.3%)	
1	56 (35.9%)	41 (37.6%)	15 (31.9%)	
2	26 (16.7%)	12 (11.0%)	6 (12.8%)	
LVI				1
Negative	96 (61.5%)	67 (61.5%)	29 (61.7%)	
Positive	60 (38.5%)	42 (38.5%)	18 (38.3%)	
PNI				0.038
Negative	22 (14.1%)	20 (18.3%)	2 (4.3%)	
Positive	134 (85.9%)	89 (81.7%)	45 (95.7%)	
Ki-67				0.539
≥50%	132 (84.6%)	94 (86.2%)	38 (80.9%)	
<50%	24 (15.4%)	15 (13.8%)	9 (19.1%)	
SMAD4 expression				0.448
Negative	95 (60.9%)	69 (63.3%)	26 (55.3%)	
Positive	61 (39.1%)	40 (36.7%)	21 (44.7%)	
Clavien-Dindo classification				0.476
0	108 (69.2%)	73 (67.0%)	35 (74.5%)	
I–II	46 (29.5%)	35 (32.1%)	11 (23.4%)	
III–V	2 (1.3%)	1 (0.9%)	1 (2.1%)	
Adjuvant therapy regimen				0.042
Gemcitabine-based	89 (57.1%)	62 (56.9%)	27 (57.4%)	
5FU-based	53 (34.0%)	41 (37.6%)	12 (25.5%)	
Combining	14 (8.9%)	6 (5.5%)	8 (17.0%)	
Duration of adjuvant therapy				0.544
<two cycles	53 (34.0%)	36 (33.0%)	17 (36.2%)	
two to four cycles	40 (25.6%)	26 (23.9%)	14 (29.8%)	

(Continued)

TABLE 1 | Continued

Variables	Overall (N = 156)	Training cohort (N = 109)	Validation cohort (N = 47)	P
Recurrence site	63 (40.4%)	47 (43.1%)	16 (34.0%)	0.257
four to six cycles				
Local	15 (9.6%)	12 (11.0%)	3 (6.4%)	
Liver	30 (19.2%)	24 (22.0%)	6 (12.8%)	
Peritoneum	11 (7.1%)	7 (6.4%)	4 (8.5%)	
Multiple sites	27 (17.3%)	21 (19.3%)	6 (12.8%)	
Other or uncertain sites	23 (14.7%)	16 (14.7%)	7 (14.9%)	0.591
None	50 (32.1%)	29 (26.6%)	21 (44.7%)	
Rad-score				0.591
High	50 (32.1%)	33 (30.3%)	17 (36.2%)	
Low	106 (67.9%)	76 (69.7%)	30 (63.8%)	0.214
Total risk score				
High	29 (18.6%)	18 (16.5%)	11 (23.4%)	
Intermediate	44 (28.2%)	28 (25.7%)	16 (34.0%)	
Low	83 (53.2%)	63 (57.8%)	20 (42.6%)	

BMI, body mass index; DP, distal pancreatectomy; PD, pancreatoduodenectomy; TP, total pancreatectomy; NLR, neutrophil-to-lymphocyte ratio; PLR, platelet-to-lymphocyte ratio; LVI, lymphovascular invasion; PNI, perineural invasion.

preoperative levels. Positive surgical margins were found in 32 patients (20.5%), and SMAD4 immunohistochemical staining was confirmed as positive in 61 patients (39.1%). PNI and adjuvant therapy regimens were significantly different between the training and validation sets ($p = 0.038$ and $p = 0.042$, respectively). The other clinical features were not significantly different between the groups. Regarding the recurrence pattern of RPC, the most frequent site of recurrence following pancreatectomy for PDAC was the liver. Most patients had recurrence at distant sites, either isolated or multiple sites ($n = 91$; 58.3%), while liver-only recurrence was found in 30 patients (19.2%), and isolated local recurrence in 15 patients (9.6%). The details of the baseline data are summarized in **Table 1**.

Feature Extraction and Construction of the Rad-Score

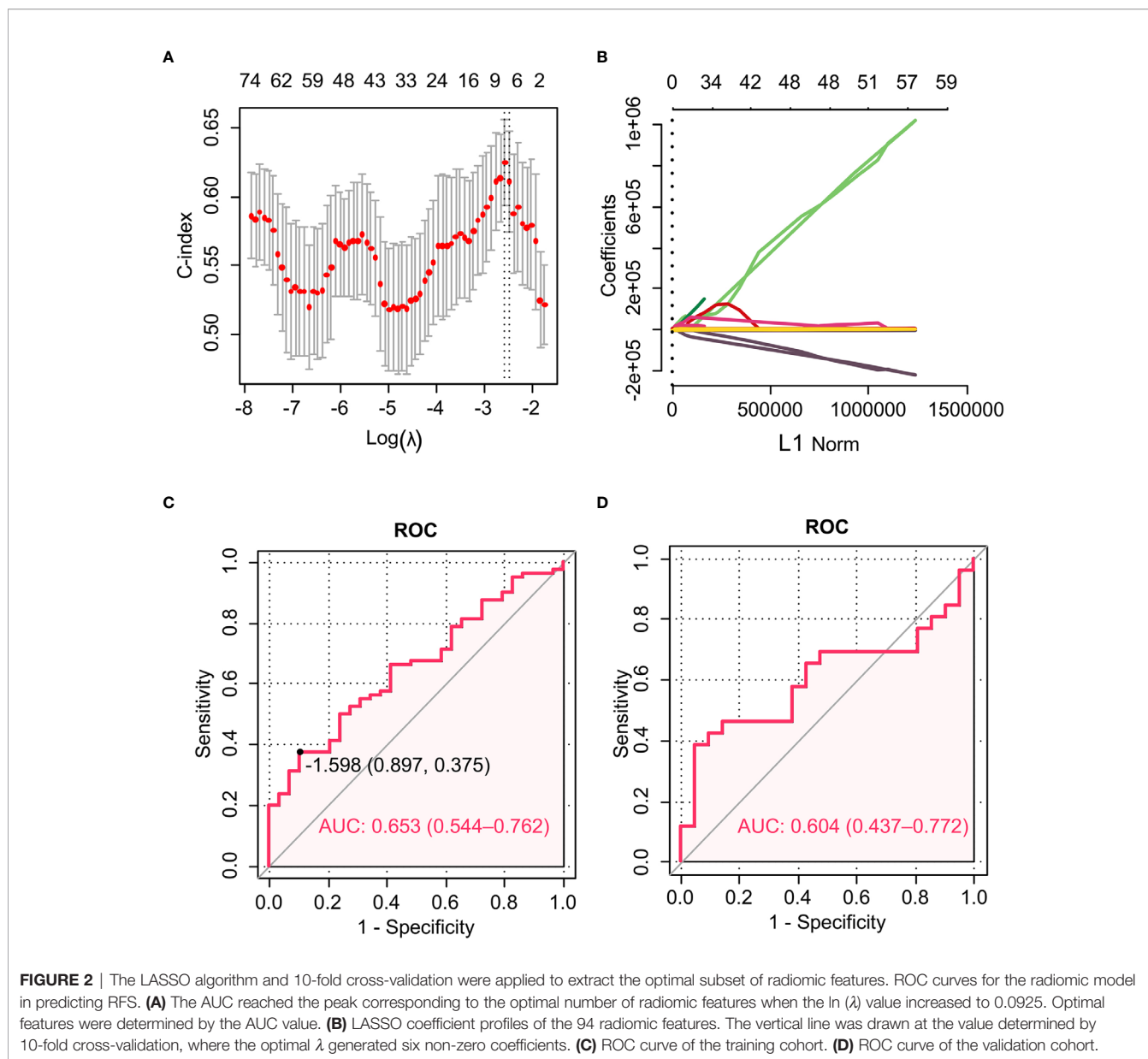
Using the LASSO algorithm and 10-fold cross-validation, we extracted the optimal subset of radiomic features. The value of 0.0925 was determined as the optimal λ , and eventually six of 94 radiomic features with non-zero coefficients were chosen in the training set (**Figures 2A, B**). The six selected radiomic features were $PETGLZLM_{LZE}$, $PETSHAPE_{Sphericity}$, $PETCONVENTIONAL_{SUVbwSkewness}$, $CTSHAPE_{Sphericity}$, $CTSHAPE_{Compacity}$, and $CTCONVENTIONAL_{HUSkewness}$. Among the six features, the first three were related to PET, while the remaining three features were derived from CT imaging. To calculate the rad-score of each patient, we constructed a logistic regression formula containing the above selected features as follows: $rad-score = PETGLZLM_{LZE} \times 7.84 \times 10^{-6} - PETSHAPE_{Sphericity} \times 1.354944481 - PETCONVENTIONAL_{SUVbwSkewness} \times 0.219952725 - CTCONVENTIONAL_{HUSkewness} \times 0.078539806 - CTSHAPE_{Sphericity} \times 0.629610997 - CTSHAPE_{Compacity} \times 0.073882711$. In this formula, element (i, j) of $GLZLM$ corresponds to the number of homogeneous zones of j voxels with the intensity i in an image and is called $GLZLM(i, j)$ thereafter. $GLZLM_{LZE} = \frac{1}{H} \sum_i \sum_j GLZLM(i, j) \cdot j^2$, where H corresponds to the number of homogeneous zones in the VOI. $SHAPE_{Sphericity} = \frac{\pi^{1/3} \cdot (6V)^{2/3}}{A}$, $SHAPE_{Compacity} =$

$\frac{A^{3/2}}{V}$, Where V and A correspond to the volume and the surface of the VOI based on the Delaunay triangulation. $CONVENTIONAL_{Skewness} = \frac{\frac{1}{N} \sum_i i(I(i)-\bar{I})^3}{(\sqrt{\frac{1}{N} \sum_i (I(i)-\bar{I})^2})^3}$, where $I(i)$ corresponds to the number of voxels with intensity i, N the total number of voxels in the VOI and \bar{I} the average of gray-levels.

To evaluate the performance of the selected radiomic features in predicting the RFS of RPC patients, ROC curves were used. The rad-score had AUCs of 0.653 (95% CI, 0.544–0.762) in the training set and 0.604 (95% CI, 0.437–0.772) in the validation cohort (**Figures 2C, D**). The cutoff value of the rad-score was -1.598 . The C-indexes of the difference in the probability of survival between the high and low rad-score groups in the training and validation cohorts were 0.784 (95% CI, 0.693–0.875) and 0.836 (95% CI, 0.713–0.959), respectively. Kaplan-Meier survival curves for the high and low rad-score groups in the training and validation cohort were depicted (**Figures 3A, B**). Waterfall plots were drawn to display the rad-score of each patient (**Figure S2A**).

Development and Validation of a Risk Stratification System for Recurrence Prediction

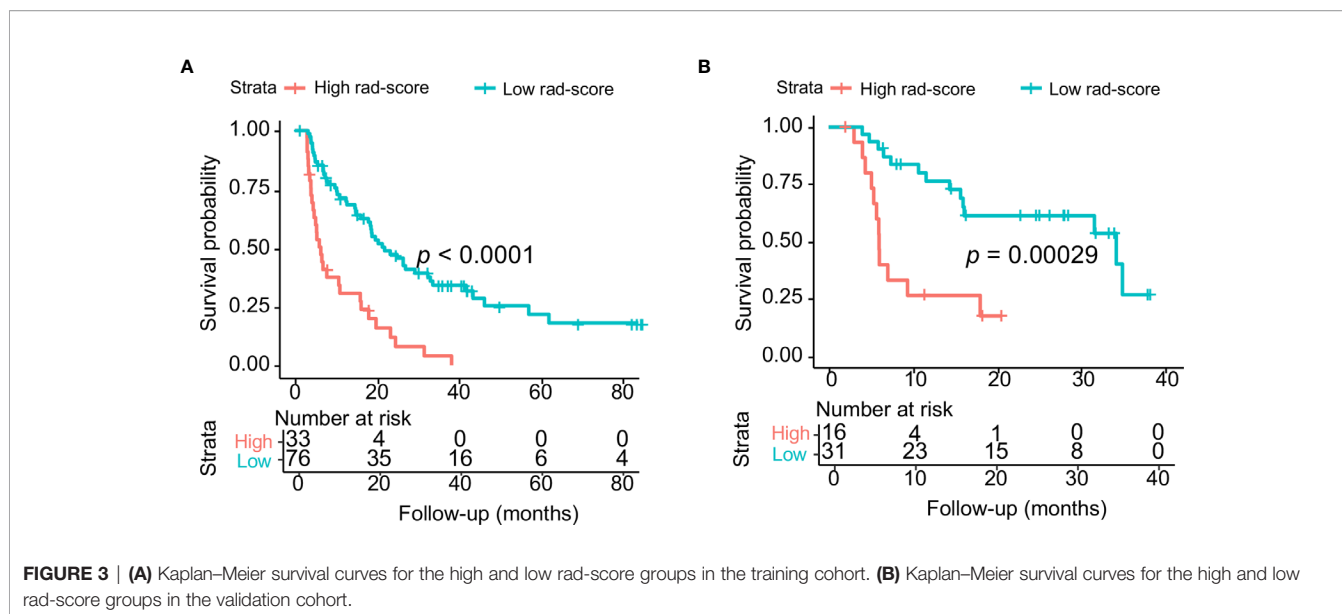
Each clinicopathological factor was converted into a categorical variable, and then we performed univariate and multivariable Cox analyses to determine the independent risk factors for recurrence in PDAC patients who had undergone surgery. Variables with $P < 0.05$ in the univariate analysis were further incorporated into multivariable Cox analysis including the following factors: rad-score (high vs low), tumor differentiation (low vs moderate-high), lymph node metastasis (positive vs negative), $\Delta CA19-9$ ($<80\%$ decrease vs $\geq 80\%$ decrease), LVI (positive vs negative), SMAD4 expression (negative vs positive) and duration of adjuvant therapy ($<two$ vs two to $four$ vs $four$ to six cycles). The results of multivariable Cox analysis revealed that the rad-score, $\Delta CA19-9$ and duration of adjuvant therapy were three independent risk factors for recurrence in PDAC patients who had undergone resection [rad-score: HR, 2.891, (95% CI,



1.704–4.905; $P < 0.001$); $\Delta\text{CA19-9}$: HR, 1.842, (95% CI, 1.088–3.118; $P = 0.023$); and duration of adjuvant therapy: two to four cycles HR, 1.703, (95% CI, 0.904–3.206), <two cycles HR, 2.388, (95% CI, 1.161–4.909; $P < 0.001$) (Table 2). Independent risk factors were selected to establish a recurrence prediction model, the risk stratification system. The score was calculated according to the six prognostic predictors weighted by β regression coefficients in multivariable Cox analysis, which were rounded into integer values using the method by Sullivan et al. (22): 11 points for a high rad-score, nine points for four to six cycles of adjuvant chemotherapy, seven points for low differentiation, six points for $\geq 80\%$ decrease in $\Delta\text{CA19-9}$, five points for <two cycles of adjuvant chemotherapy, three points for positive LVI, three points for lymph node metastasis, and one point for positive SMAD4 expression. The total risk score ranged from 0 to 40

points. According to X-tile analysis, 16 and 29 points were used as the cutoff values, 64 (58.72%), 34 (31.19%), and 11 patients (10.09%) were categorized into the low- (0 to 16), intermediate- (17 to 29), and high-risk (30 to 40) groups, respectively. The results of the validation cohort were similar: there were 51.1, 31.9, and 17.0% of the patients in the low-, medium-, and high-risk group, respectively. Waterfall plots were drawn according to the risk score (Figure S2B).

To predict the one-year recurrence risk, the Brier scores of the final model (rad-score + $\Delta\text{CA19-9} \geq 80\%$ decrease + tumor differentiation + lymph node metastasis + LVI + SMAD4 expression + adjuvant chemotherapy) in the training and validation cohorts were 0.14 and 0.20, which corresponded to IPA values of 30.6 and 20.6%, respectively. Table 3 indicates the changes in the Brier score and IPA at 1 year regarding RFS when



each of the seven variables was excluded from the model, suggesting that the incorporation of these seven variables in the final model was favorable to optimize the prediction accuracy of the risk stratification system.

The prediction accuracy of this risk stratification system for PDAC recurrence, evaluated by the C-index, was 0.890 (95% CI, 0.835–0.945) for the training cohort and 0.865 (95% CI, 0.778–0.952) for the validation cohort. The 1-year RFS rates of the low-, intermediate-, and high-risk groups were 85.5, 24.0, and 9.1%,

respectively (**Figure 4A**). In the validation cohort, the 1-year survival rates in the low-, intermediate-, and high-risk groups were 86.7, 38.9, and 14.3%, respectively (**Figure 4B**). In this study, the median follow-up time was 24.8 months (range, 3 to 84.8 months), and survival data were obtained to explore the prognostic value of risk stratification. In the training cohort, patients in the high-risk group (n = 11) showed significantly shorter survival times than those in the low-risk (n = 64) and intermediate-risk groups (n = 34) (P < 0.0001; **Figure 4C**).

TABLE 2 | Construction of a risk-stratification system for risk stratification in RPC patients.

Variables	Univariate analysis	Multivariate analysis	HR (95% CI)	β-Coefficient	Score assigned
	P	P			
Rad-score	<0.001	<0.001			
Low			Reference group	.	0
High			2.891 (1.704–4.905)	1.062	11
Differentiation	<0.001	0.065			
Median-high			Reference group	.	0
Low			2.103 (0.955–4.63)	0.743	7
Lymph node metastasis	0.001	0.3			
Negative			Reference group	.	0
Positive			1.312 (0.785–2.193)	0.272	3
ΔCA19-9 decrease	0.001	0.023			
≥ 80%			Reference group	.	0
< 80%			1.842 (1.088–3.118)	0.611	6
LVI	0.001	0.302			
Negative			Reference group	.	0
Positive			1.296 (0.792–2.12)	0.259	3
SMAD4 expression	0.036	0.633			
Positive			Reference group	.	0
Negative			1.145 (0.657–1.997)	0.136	1
Adjuvant chemotherapy		< 0.001			
four to six cycles			Reference group	.	0
two to four cycles	0.0116	0.099	1.703 (0.904–3.206)	0.532	5
<two cycles	<0.001	0.018	2.388 (1.161–4.909)	0.87	9

LVI, lymphovascular invasion.

TABLE 3 | Comparison of the different models regarding RFS in the training and validation cohorts.

No. of Variables	Variables included in the model	Brier score	IPA at 1year, %	IPA drop
Training cohort				
1 (final model)	Rad-score + Δ CA19-9 + Differentiation + Lymph node metastasis + LVI + SMAD4 + Adjuvant therapy	0.135551151	0.305826195	0
2	Δ CA19-9 + Differentiation + Lymph node metastasis + LVI + SMAD4 + Adjuvant therapy	0.139392659	0.286153371	0.019672824
3	Rad-score + Δ CA19-9 + Lymph node metastasis + LVI + SMAD4 + Adjuvant therapy	0.146757759	0.248435803	0.057390392
4	Rad-score + Δ CA19-9 + Differentiation + LVI + SMAD4 + Adjuvant therapy	0.136588037	0.300516179	0.005310016
5	Rad-score + Differentiation + Lymph node metastasis + LVI + SMAD4 + Adjuvant therapy	0.144486321	0.260068112	0.045758083
6	Rad-score + Δ CA19-9 + Differentiation + Lymph node metastasis + SMAD4 + Adjuvant therapy	0.143317882	0.26605183	0.039774365
7	Rad-score + Δ CA19-9 + Differentiation + Lymph node metastasis + LVI + Adjuvant therapy	0.14245439	0.270473875	0.03535232
8	Rad-score + Δ CA19-9 + Differentiation + Lymph node metastasis + LVI	0.138483372	0.290809936	0.015016259
Validation cohort				
1 (final model)	Rad-score + Δ CA19-9 + Differentiation + Lymph node metastasis + LVI + SMAD4 + Adjuvant therapy	0.196208964	0.206180219	0
2	Δ CA19-9 + Differentiation + Lymph node metastasis + LVI + SMAD4 + Adjuvant therapy	0.19784561	0.199558697	0.006621522
3	Rad-score + Δ CA19-9 + Lymph node metastasis + LVI + SMAD4 + Adjuvant therapy	0.198989105	0.194932359	0.01124786
4	Rad-score + Δ CA19-9 + Differentiation + LVI + SMAD4 + Adjuvant therapy	0.19977719	0.191743931	0.014436288
5	Rad-score + Differentiation + Lymph node metastasis + LVI + SMAD4 + Adjuvant therapy	0.222610612	0.099364758	0.106815461
6	Rad-score + Δ CA19-9 + Differentiation + Lymph node metastasis + SMAD4 + Adjuvant therapy	0.200846238	0.187418792	0.018761427
7	Rad-score + Δ CA19-9 + Differentiation + Lymph node metastasis + Adjuvant therapy	0.19950763	0.192834516	0.013345703
8	Rad-score + Δ CA19-9 + Differentiation + Lymph node metastasis + LVI	0.200743146	0.187835881	0.018344337

Δ CA19-9 indicates a level decrease $\geq 80\%$; SMAD4 indicates a negative status; and the duration of adjuvant therapy was divided into three categories: <two cycles, two to four cycles, and four to six cycles.

A similar trend was observed in the validation cohort risk group ($P < 0.0001$; **Figure 4D**).

DISCUSSION

This study presents an internally validated risk stratification system for predicting early relapse in patients with resected pancreatic cancer. Integrating preoperative ^{18}F -PET/CT radiomic features, changes in a sensitive biomarker (Δ CA19-9), pathological characteristics (tumor differentiation, lymph node metastasis, LVI, and SMAD4 expression), and the duration of adjuvant chemotherapy associated with early recurrence, the patients were scored ranging from 0 to 40. Herein, we classified patients into three groups with corresponding points assigned as follows: low-risk group (0–16 points), intermediate-risk group (17–29 points), and high-risk group (30–40 points). Compared with low-risk patients, the relapse rate was two to three times higher in the intermediate-risk group and six to nine times higher in the high-risk group. Our risk stratification system was confirmed to stratify patients by increasing risk of recurrence accurately in an independent internally validation cohort. Accordingly, we recommend that patients in the high- and intermediate-risk groups be followed-up for recurrence at regular intervals, such as every 2–3 months.

The six selected radiomic features were used to construct a formula of rad-score calculation. The *GLZLM* provides information on the size of homogeneous zones for each gray-level in three dimensions. From this matrix, 11 texture indices are computed. More precisely, *GLZLM* is particularly efficient to characterize the texture homogeneity, which had provided better characterizations than *GLRLM* or *GLCM* for the classification of textures in PET images. *SHAPE_Sphericity* and *SHAPE_Compacity* reflect how spherical and compact the VOI

is. Sphericity is a measure of the roundness of the shape of the tumor region relative to a sphere and is equal to 1 for a perfect sphere. *CONVENTIONAL_Skewness* measures the asymmetry of the gray-level distribution. Depending on where the tail is elongated and the mass of the distribution is concentrated, this value can be positive or negative. Fiorino et al. (25) established a radiomic-based index with good performance derived from ^{18}F -FDG PET/CT radiomics features to predict distant RFS in 176 patients with locally advanced pancreatic cancer treated with radio-chemotherapy. In their study, one-hundred-ninety-eight radiomic features were extracted, and only two robust features were included, *Morphological_COMshift* and *Statistical_P₁₀*. Specifically, the *COMshift* is the distance between the VOI centroid and the intensity-weighted VOI centroid. *P₁₀* is an intensity-based statistical feature which represents the 10th percentile of the set of gray levels of the voxels included in the VOI. Exploration of CT-based radiomics to predict survival prognosis or treatment response in pancreatic cancer is more common (14, 17, 18). Researcher also developed a multiparametric MRI radiomic nomogram for preoperative evaluation of early recurrence risks in resectable pancreatic cancer, incorporating the radiomic signatures from T1-w, T2-w, portal venous phase, and arterial phase and clinical parameters (26). Recently, radiogenomics is an emerging field that integrates “radiomics” and “genomics”, which may aid in the development of precision medicine. Iwatate et al. (27) found that radiogenomics could predict p53 mutations and in turn the prognosis of PDAC patients. Pancreatic cancer remains one of the most lethal malignancies, radiomics may have the potential to address some problems but further validation in larger-scale, multicenter studies and in randomized control trials is required.

In PDAC, the median survival of surgery-only patients is 15–20 months, and the 5-year survival rate is 8–15% (28–31). Even after curative resection, 69–75% of patients with pancreatic cancer show recurrence within 2 years (28–30, 32, 33). Clinicopathological

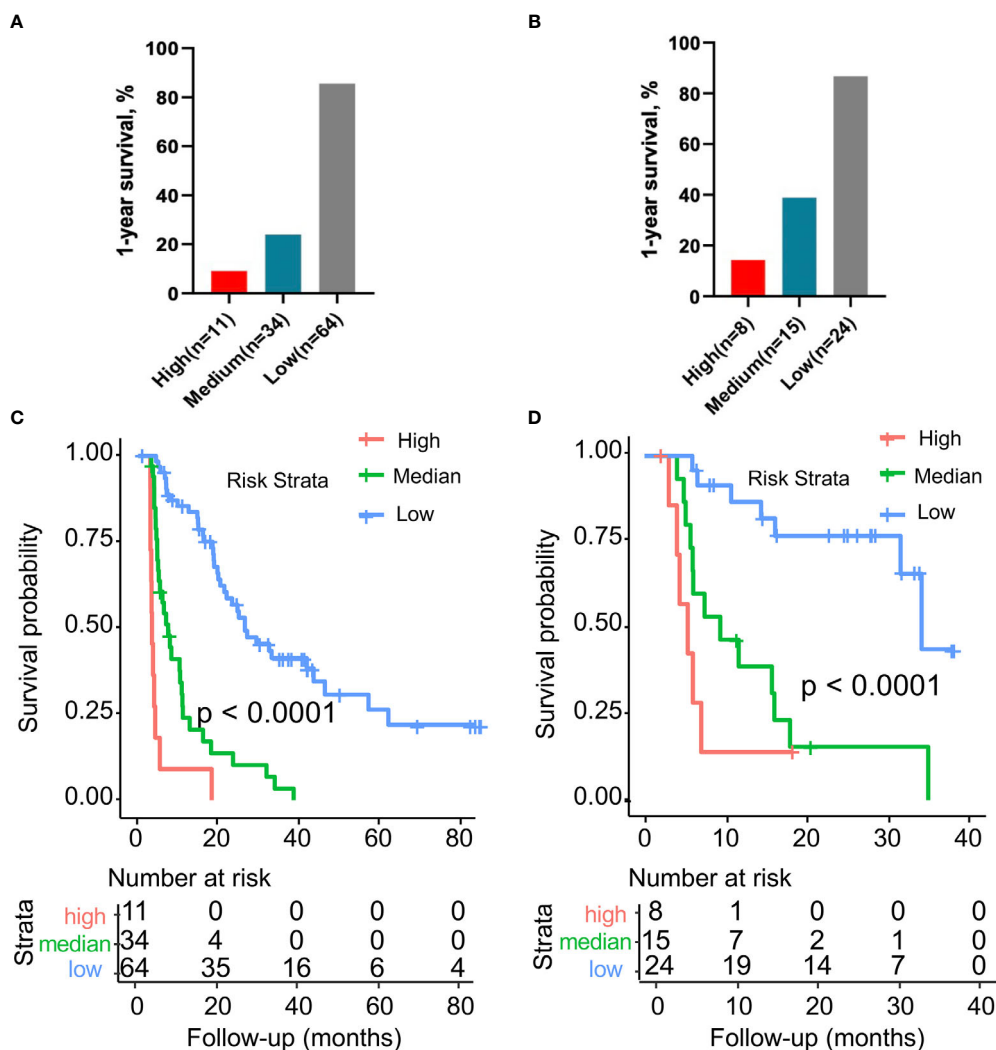


FIGURE 4 | (A) Comparison of the 1-year recurrence-free survival rate in the training cohort with different risk stratifications. **(B)** Comparison of the 1-year recurrence-free survival rate in the validation cohort with different risk stratifications. **(C)** Kaplan–Meier survival curves for the three risk stratification groups in the training cohort. **(D)** Kaplan–Meier survival curves for the three risk stratification groups in the validation cohort. Risk stratification system: low risk, 0 to 16 points; medium risk, 17 to 29 points; high risk, 30 to 40 points.

parameters, including tumor differentiation, lymph node metastasis, and LVI, were found to be strong predictors of prognosis in PDAC patients who had undergone surgical resection (3, 34–36). The NLR and PLR are inflammatory indicators that are correlated with OS in PDAC patients (21, 37–39). The Ki-67 proliferative index could be used in the survival prediction of resectable PDAC, and an index above 50% was negatively related to survival compared with other patients (20). However, the above indices showed no predictive value for recurrence in our study.

CA19-9 is the most studied efficacy predictor and prognostic biomarker in PDAC (40, 41). Patients with preoperative CA19-9 $\geq 1,000$ U/ml generally showed a poor surgical benefit; however, subgroups with CA19-9 levels decreased postoperatively may still achieve a survival benefit. For borderline or locally advanced PDAC patients, the CA19-9 response (reduction $>50\%$) during

primary or neoadjuvant chemotherapy may provide insight into a patient selection that will benefit from surgical resection (42–44). However, Tsai et al. (45) retrospectively analyzed 131 PDAC patients and suggested that following neoadjuvant therapy, CA19-9 normalization is a robust prognostic factor for longer survival. In this study, we found that a reduction in the CA19-9 levels of $\geq 80\%$ after resection indicated a better prognosis. SMAD4 is a widely known tumor suppressor that is inactivated in more than half of PDAC patients (46). SMAD4 deficiency induced by genomic deletions or truncated mutations are associated with an inferior prognosis in pancreatic cancer (47). Our results demonstrated a SMAD4 negative status is independently significantly correlated with RFS in PDAC patients.

The high relapse rate of pancreatic cancer following curative surgery suggests the necessity of adjuvant therapy. Currently,

the regimens are based on 5-FU or gemcitabine, and a combination chemotherapy with gemcitabine and capecitabine or mFOLFIRINOX has been verified to improve OS (48, 49). We retrospectively analyzed the duration of adjuvant treatment grouped into three categories (without or <2 months, 2–4 months, and 4–6 months) and found that a longer duration conferred benefit to RPC patients, demonstrating the adequate adjuvant course for the high recurrence risk population, and may present a potentially promising treatment option of consolidation therapy in pancreatic cancer patients. Most of the patients in our study initiated adjuvant therapy within eight weeks postoperatively according to the current consensus (50), and previous results showed that patients still benefit from adjuvant therapy started more than 12 weeks after surgical resection (51).

From 2013, eligible patients were continuously recruited, and our study may present as one of the largest sample sizes published in pancreatic cancer to date. The follow-up duration ranged from 3 to 84.8 months. Our results showed that the recurrence risk stratification system had good predictive performance. Nevertheless, our study has many limitations. First, selection bias exists as a potential flaw inherent in retrospective analysis. Prospective multi-center studies on ¹⁸F-FDG PET/CT of resected PDAC are needed to limit the bias and verify whether certain features could work as reliable predictors. Second, our research discussed only the predictive performance of the model for patients undergoing surgical resection, but the intratumoral heterogeneity of pancreatic cancer should be further studied. Third, evidence from ESPAC-4 and PRODIGE24/CCTG PA.6 demonstrated that the adjuvant combination of gemcitabine and capecitabine, or modified FOLFIRINOX regimens, shows longer survival than gemcitabine alone in resected pancreatic cancer patients (31, 49). Nearly all the patients in our study used gemcitabine or 5-FU mono-chemotherapy on account of the time of consultation. Better survival could be achieved when patients received new combination regimen.

CONCLUSION

The risk stratification system based on ¹⁸F-FDG PET/CT radiomic features demonstrated good performance in relapse prediction after pancreatectomy in RPC patients, providing strong recommendations for adequate adjuvant therapy courses, particularly for patients with a high risk of relapse, and maybe a useful method for monitoring and surveillance in a clinical setting.

REFERENCES

1. Siegel RL, Miller KD, Jemal A. Cancer Statistics, 2020. *CA Cancer J Clin* (2020) 70(1):7–30. doi: 10.3322/caac.21590
2. Ducreux M, Cuhna AS, Caramella C, Hollebecque A, Burtin P, Goere D, et al. Cancer of the Pancreas: ESMO Clinical Practice Guidelines for Diagnosis, Treatment and Follow-Up. *Ann Oncol* (2015) 26 Suppl 5:v56–68. doi: 10.1093/annonc/mdv295
3. Groot VP, Gemenetzi G, Blair AB, Rivero-Soto RJ, Yu J, Javed AA, et al. Defining and Predicting Early Recurrence in 957 Patients With Resected Pancreatic Ductal Adenocarcinoma. *Ann Surg* (2019) 269(6):1154–62. doi: 10.1097/SLA.0000000000002734
4. Neuzillet C, Gaujoux S, Williet N, Bachet JB, Baugeon L, Colson Durand L, et al. Pancreatic Cancer: French Clinical Practice Guidelines for Diagnosis, Treatment and Follow-Up (SNFGE, FFCD, Gercor, UNICANCER, Sfd, SFED, Sfro, ACHBT, Afc). *Dig Liver Dis* (2018) 50(12):1257–71. doi: 10.1016/j.dld.2018.08.008
5. Chu LC, Goggins MG, Fishman EK. Diagnosis and Detection of Pancreatic Cancer. *Cancer J* (2017) 23(6):333–42. doi: 10.1097/PPO.0000000000000290

DATA AVAILABILITY STATEMENT

The original contributions presented in the study are included in the article/**Supplementary Material**. Further inquiries can be directed to the corresponding authors.

ETHICS STATEMENT

The studies involving human participants were reviewed and approved by the Ethics Committee of the Fudan University Shanghai Cancer Center. The patients/participants provided their written informed consent to participate in this study.

AUTHOR CONTRIBUTIONS

MW, BG, and SS conceptualized and designed the study. SLS, BZ WW, JX, and XY performed analysis. XY and SS interpreted the data. MW and BG drafted the manuscript. XY and SS revised the manuscript. All authors contributed to the article and approved the submitted version.

FUNDING

This study was jointly funded by the National Natural Science Foundation of China (No. 81772555, 81802352 and 81902428), the National Science Foundation for Distinguished Young Scholars of China (No. 81625016), the Shanghai Sailing Program (No. 19YF1409400 and 20YF1409000), the Shanghai Rising-Star Program (No. 20QA1402100), the Shanghai Anticancer Association Young Eagle Program (No.SACA-CY19A06), the Clinical and Scientific Innovation Project of Shanghai Hospital Development Center (No. SHDC12018109 and SHDC12019109) the Clinical Research Plan of SHDC (No.SHDC2020CR1006A), and the Scientific Innovation Project of Shanghai Education Committee (No. 2019-01-07-00-07-E00057).

SUPPLEMENTARY MATERIAL

The Supplementary Material for this article can be found online at: <https://www.frontiersin.org/articles/10.3389/fonc.2021.650266/full#supplementary-material>

6. Daamen LA, Groot VP, Goense L, Wessels FJ, Borel Rinkes IH, Intven MPW, et al. The Diagnostic Performance of CT Versus FDG PET-CT for the Detection of Recurrent Pancreatic Cancer: A Systematic Review and Meta-Analysis. *Eur J Radiol* (2018) 106:128–36. doi: 10.1016/j.ejrad.2018.07.010
7. Heinrich S, Goerres GW, Schafer M, Sagmeister M, Bauerfeind P, Pestalozzi BC, et al. Positron Emission Tomography/Computed Tomography Influences on the Management of Resectable Pancreatic Cancer and its Cost-Effectiveness. *Ann Surg* (2005) 242(2):235–43. doi: 10.1097/01.sla.0000172095.97787.84
8. Zhang A, Ren S, Yuan Y, Li X, Zhu X, Jiang L, et al. Prognostic Values of ¹⁸F-FDG PET/CT Metabolic Parameters and Clinical Figures in Locally Advanced Pancreatic Cancer Underwent Chemotherapy Combined With Stereotactic Body Radiation Therapy. *Med (Baltimore)* (2019) 98(13):e15064. doi: 10.1097/MD.00000000000015064
9. Yokose T, Kitago M, Matsusaka Y, Masugi Y, Shinoda M, Yagi H, et al. Usefulness of (18) F-fluorodeoxyglucose Positron Emission Tomography/Computed Tomography for Predicting the Prognosis and Treatment Response of Neoadjuvant Therapy for Pancreatic Ductal Adenocarcinoma. *Cancer Med* (2020) 9(12):4059–68. doi: 10.1002/cam4.3044
10. Halbrook CJ, Lyssiottis CA. Employing Metabolism to Improve the Diagnosis and Treatment of Pancreatic Cancer. *Cancer Cell* (2017) 31(1):5–19. doi: 10.1016/j.ccell.2016.12.006
11. Pimiento JM, Davis-Yadley AH, Kim RD, Chen DT, Eikman EA, Berman CG, et al. Metabolic Activity by ¹⁸F-FDG-PET/CT Is Prognostic for Stage I and II Pancreatic Cancer. *Clin Nucl Med* (2016) 41(3):177–81. doi: 10.1097/RLU.0000000000001098
12. Fisher R, Pusztai L, Swanton C. Cancer Heterogeneity: Implications for Targeted Therapeutics. *Br J Cancer* (2013) 108(3):479–85. doi: 10.1038/bjc.2012.581
13. Hatt M, Le Rest CC, Tixier F, Badic B, Schick U, Visvikis D. Radiomics: Data are Also Images. *J Nucl Med* (2019) 60(Suppl 2):38S–44S. doi: 10.2967/jnumed.118.220582
14. Parr E, Du Q, Zhang C, Lin C, Kamal A, McAlister J, et al. Radiomics-Based Outcome Prediction for Pancreatic Cancer Following Stereotactic Body Radiotherapy. *Cancers (Basel)* (2020) 12(4):1051. doi: 10.3390/cancers12041051
15. Xie T, Wang X, Li M, Tong T, Yu X, Zhou Z. Pancreatic Ductal Adenocarcinoma: A Radiomics Nomogram Outperforms Clinical Model and TNM Staging for Survival Estimation After Curative Resection. *Eur Radiol* (2020) 30(5):2513–24. doi: 10.1007/s00330-019-06600-2
16. Lim CH, Cho YS, Choi JY, Lee KH, Lee JK, Min JH, et al. Imaging Phenotype Using (18)F-Fluorodeoxyglucose Positron Emission Tomography-Based Radiomics and Genetic Alterations of Pancreatic Ductal Adenocarcinoma. *Eur J Nucl Med Mol Imaging* (2020) 47(9):2113–22. doi: 10.1007/s00259-020-04698-x
17. Nasief H, Hall W, Zheng C, Tsai S, Wang L, Erickson B, et al. Improving Treatment Response Prediction for Chemoradiation Therapy of Pancreatic Cancer Using a Combination of Delta-Radiomics and the Clinical Biomarker Ca19-9. *Front Oncol* (2019) 9:1464. doi: 10.3389/fonc.2019.01464
18. Nasief H, Zheng C, Schott D, Hall W, Tsai S, Erickson B, et al. A Machine Learning Based Delta-Radiomics Process for Early Prediction of Treatment Response of Pancreatic Cancer. *NPJ Precis Oncol* (2019) 3:25. doi: 10.1038/s41698-019-0096-z
19. Kadera BE, Sunjaya DB, Isacoff WH, Li L, Hines OJ, Tomlinson JS, et al. Locally Advanced Pancreatic Cancer: Association Between Prolonged Preoperative Treatment and Lymph-Node Negativity and Overall Survival. *JAMA Surg* (2014) 149(2):145–53. doi: 10.1001/jamasurg.2013.2690
20. Pergolini I, Crippa S, Pagnanelli M, Belfiori G, Pucci A, Partelli S, et al. Prognostic Impact of Ki-67 Proliferative Index in Resectable Pancreatic Ductal Adenocarcinoma. *BJS Open* (2019) 3(5):646–55. doi: 10.1002/bjs.5.0175
21. Gemenetzi G, Bagante F, Griffin JF, Rezaee N, Javed AA, Manos LL, et al. Neutrophil-to-Lymphocyte Ratio is a Predictive Marker for Invasive Malignancy in Intraductal Papillary Mucinous Neoplasms of the Pancreas. *Ann Surg* (2017) 266(2):339–45. doi: 10.1097/SLA.0000000000001988
22. Sullivan LM, Massaro JM, D'Agostino RBSR. Presentation of Multivariate Data for Clinical Use: The Framingham Study Risk Score Functions. *Stat Med* (2004) 23(10):1631–60. doi: 10.1002/sim.1742
23. Kattan MW, Gerds TA. The Index of Prediction Accuracy: An Intuitive Measure Useful for Evaluating Risk Prediction Models. *Diagn Progn Res* (2018) 2:7. doi: 10.1186/s41512-018-0029-2
24. Camp RL, Dolled-Filhart M, Rimm DL. X-Tile: A New Bio-Informatics Tool for Biomarker Assessment and Outcome-Based Cut-Point Optimization. *Clin Cancer Res* (2004) 10(21):7252–9. doi: 10.1158/1078-0432.CCR-04-0713
25. Mori M, Passoni P, Incerti E, Bettinardi V, Broggi S, Reni M, et al. Training and Validation of a Robust PET Radiomic-Based Index to Predict Distant-Relapse-Free-Survival After Radio-Chemotherapy for Locally Advanced Pancreatic Cancer. *Radiother Oncol* (2020) 153:258–64. doi: 10.1016/j.radonc.2020.07.003
26. Tang TY, Li X, Zhang Q, Guo CX, Zhang XZ, Lao MY, et al. Development of a Novel Multiparametric MRI Radiomic Nomogram for Preoperative Evaluation of Early Recurrence in Resectable Pancreatic Cancer. *J Magn Reson Imaging* (2020) 52(1):231–45. doi: 10.1002/jmri.27024
27. Iwatate Y, Hoshino I, Yokota H, Ishige F, Itami M, Mori Y, et al. Radiogenomics for Predicting p53 Status, PD-L1 Expression, and Prognosis With Machine Learning in Pancreatic Cancer. *Br J Cancer* (2020) 123(8):1253–61. doi: 10.1038/s41416-020-0997-1
28. Neoptolemos JP, Stocken DD, Friess H, Bassi C, Dunn JA, Hickey H, et al. A Randomized Trial of Chemoradiotherapy and Chemotherapy After Resection of Pancreatic Cancer. *N Engl J Med* (2004) 350(12):1200–10. doi: 10.1056/NEJMoa032295
29. Neoptolemos JP, Stocken DD, Tudur Smith C, Bassi C, Ghaneh P, Owen E, et al. Adjuvant 5-Fluorouracil and Folinic Acid vs Observation for Pancreatic Cancer: Composite Data From the ESPAC-1 and -3(v1) Trials. *Br J Cancer* (2009) 100(2):246–50. doi: 10.1038/sj.bjc.6604838
30. Oettle H, Post S, Neuhaus P, Gellert K, Langrehr J, Ridwelski K, et al. Adjuvant Chemotherapy With Gemcitabine vs Observation in Patients Undergoing Curative-Intent Resection of Pancreatic Cancer: A Randomized Controlled Trial. *JAMA* (2007) 297(3):267–77. doi: 10.1001/jama.297.3.267
31. Neoptolemos JP, Palmer DH, Ghaneh P, Psarelli EE, Valle JW, Halloran CM, et al. Comparison of Adjuvant Gemcitabine and Capecitabine With Gemcitabine Monotherapy in Patients With Resected Pancreatic Cancer (ESPAC-4): A Multicentre, Open-Label, Randomised, Phase 3 Trial. *Lancet* (2017) 389(10073):1011–24. doi: 10.1016/S0140-6736(16)32409-6
32. Neoptolemos JP, Stocken DD, Bassi C, Ghaneh P, Cunningham D, Goldstein D, et al. Adjuvant Chemotherapy With Fluorouracil Plus Folinic Acid vs Gemcitabine Following Pancreatic Cancer Resection: A Randomized Controlled Trial. *JAMA* (2010) 304(10):1073–81. doi: 10.1001/jama.2010.1275
33. Sinn M, Bahra M, Liersch T, Gellert K, Messmann H, Bechstein W, et al. Conko-005: Adjuvant Chemotherapy With Gemcitabine Plus Erlotinib Versus Gemcitabine Alone in Patients After R0 Resection of Pancreatic Cancer: A Multicenter Randomized Phase III Trial. *J Clin Oncol* (2017) 35(29):3330–7. doi: 10.1200/JCO.2017.72.6463
34. Jamiyan T, Shiraki T, Kurata Y, Ichinose M, Kubota K, Imai Y. Clinical Impacts of Resection Margin Status and Clinicopathologic Parameters on Pancreatic Ductal Adenocarcinoma. *World J Surg Oncol* (2020) 18(1):137. doi: 10.1186/s12957-020-01900-0
35. Tanaka M, Mihaljevic AL, Probst P, Heckler M, Klaiber U, Heger U, et al. Meta-Analysis of Recurrence Pattern After Resection for Pancreatic Cancer. *Br J Surg* (2019) 106(12):1590–601. doi: 10.1002/bjs.11295
36. Ghaneh P, Kleeff J, Halloran CM, Raraty M, Jackson R, Melling J, et al. The Impact of Positive Resection Margins on Survival and Recurrence Following Resection and Adjuvant Chemotherapy for Pancreatic Ductal Adenocarcinoma. *Ann Surg* (2019) 269(3):520–9. doi: 10.1097/SLA.0000000000002557
37. Mei Z, Shi L, Wang B, Yang J, Xiao Z, Du P, et al. Prognostic Role of Pretreatment Blood Neutrophil-to-Lymphocyte Ratio in Advanced Cancer Survivors: A Systematic Review and Meta-Analysis of 66 Cohort Studies. *Cancer Treat Rev* (2017) 58:1–13. doi: 10.1016/j.ctrv.2017.05.005
38. Ikuta S, Sonoda T, Aihara T, Yamanaka N. A Combination of Platelet-to-Lymphocyte Ratio and Carbohydrate Antigen 19-9 Predict Early Recurrence After Resection of Pancreatic Ductal Adenocarcinoma. *Ann Transl Med* (2019) 7(18):461. doi: 10.21037/atm.2019.08.35
39. Goldstein D, El-Maraghi RH, Hammel P, Heinemann V, Kunzmann V, Sastre J, et al. nab-Paclitaxel Plus Gemcitabine for Metastatic Pancreatic Cancer: Long-Term Survival From a Phase III Trial. *J Natl Cancer Inst* (2015) 107(2):dju413. doi: 10.1093/jnci/dju413

40. Liu L, Xu H, Wang W, Wu C, Chen Y, Yang J, et al. A Preoperative Serum Signature of CEA+/CA125+/CA19-9 >/= 1000 U/mL Indicates Poor Outcome to Pancreatectomy for Pancreatic Cancer. *Int J Cancer* (2015) 136(9):2216–27. doi: 10.1002/ijc.29242
41. Xu HX, Li S, Wu CT, Qi ZH, Wang WQ, Jin W, et al. Postoperative Serum CA19-9, CEA and CA125 Predicts the Response to Adjuvant Chemoradiotherapy Following Radical Resection in Pancreatic Adenocarcinoma. *Pancreatol* (2018) 18(6):671–7. doi: 10.1016/j.pan.2018.05.479
42. Tzeng CW, Balachandran A, Ahmad M, Lee JE, Krishnan S, Wang H, et al. Serum Carbohydrate Antigen 19-9 Represents a Marker of Response to Neoadjuvant Therapy in Patients With Borderline Resectable Pancreatic Cancer. *HPB (Oxford)* (2014) 16(5):430–8. doi: 10.1111/hpb.12154
43. Boone BA, Steve J, Zenati MS, Hogg ME, Singhi AD, Bartlett DL, et al. Serum CA 19-9 Response to Neoadjuvant Therapy is Associated With Outcome in Pancreatic Adenocarcinoma. *Ann Surg Oncol* (2014) 21(13):4351–8. doi: 10.1245/s10434-014-3842-z
44. Reni M, Zanon S, Balzano G, Nobile S, Pircher CC, Chiaravalli M, et al. Selecting Patients for Resection After Primary Chemotherapy for non-Metastatic Pancreatic Adenocarcinoma. *Ann Oncol* (2017) 28(11):2786–92. doi: 10.1093/annonc/mdx495
45. Tsai S, George B, Wittmann D, Ritch PS, Krepline AN, Aldakkak M, et al. Importance of Normalization of CA19-9 Levels Following Neoadjuvant Therapy in Patients With Localized Pancreatic Cancer. *Ann Surg* (2020) 271(4):740–7. doi: 10.1097/SLA.0000000000003049
46. Iacobuzio-Donahue CA, Fu B, Yachida S, Luo M, Abe H, Henderson CM, et al. DPC4 Gene Status of the Primary Carcinoma Correlates With Patterns of Failure in Patients With Pancreatic Cancer. *J Clin Oncol* (2009) 27(11):1806–13. doi: 10.1200/JCO.2008.17.7188
47. Bardeesy N, Cheng KH, Berger JH, Chu GC, Pahler J, Olson P, et al. Smad4 is Dispensable for Normal Pancreas Development Yet Critical in Progression and Tumor Biology of Pancreas Cancer. *Genes Dev* (2006) 20(22):3130–46. doi: 10.1101/gad.1478706
48. Conroy T, Ducreux M. Adjuvant Treatment of Pancreatic Cancer. *Curr Opin Oncol* (2019) 31(4):346–53. doi: 10.1097/CCO.0000000000000546
49. Conroy T, Hammel P, Hebbar M, Ben Abdelghani M, Wei AC, Raoul JL, et al. FOLFIRINOX or Gemcitabine as Adjuvant Therapy for Pancreatic Cancer. *N Engl J Med* (2018) 379(25):2395–406. doi: 10.1056/NEJMoa1809775
50. Khorana AA, Mangu PB, Berlin J, Engebretson A, Hong TS, Maitra A, et al. Potentially Curable Pancreatic Cancer: American Society of Clinical Oncology Clinical Practice Guideline Update. *J Clin Oncol* (2017) 35(20):2324–8. doi: 10.1200/JCO.2017.72.4948
51. Ma SJ, Oladeru OT, Miccio JA, Iovoli AJ, Hermann GM, Singh AK. Association of Timing of Adjuvant Therapy With Survival in Patients With Resected Stage I to II Pancreatic Cancer. *JAMA Netw Open* (2019) 2(8):e199126. doi: 10.1001/jamanetworkopen.2019.9126

Conflict of Interest: The authors declare that the research was conducted in the absence of any commercial or financial relationships that could be construed as a potential conflict of interest.

Copyright © 2021 Wei, Gu, Song, Zhang, Wang, Xu, Yu and Shi. This is an open-access article distributed under the terms of the Creative Commons Attribution License (CC BY). The use, distribution or reproduction in other forums is permitted, provided the original author(s) and the copyright owner(s) are credited and that the original publication in this journal is cited, in accordance with accepted academic practice. No use, distribution or reproduction is permitted which does not comply with these terms.